Spin correlations and reentrant spin-glass behavior in amorphous Fe-Mn alloys: Statics

G. Aeppli
Brookhaven National Laboratory, Upton, New York 11973, and Bell Laboratories, Murray Hill, New Jersey 07974

S. M. Shapiro
Brookhaven National Laboratory, Upton, New York 11973

R. J. Birgeneau
Department of Physics, Massachusetts Institute of Technology, Cambridge, Massachusetts 02139

H. S. Chen
Bell Laboratories, Murray Hill, New Jersey 07974

(Received 14 June 1983)

Neutron scattering studies have been performed on amorphous $(Fe_{1-x}Mn_x)_{75}P_{16}B_6Al_3$ alloys for several concentrations x bracketing the spin-glass-ferromagnetic multicritical point found from magnetization measurements. The amorphous structure factor has been measured to 4.0 $Å^{-1}$, and changes considerably for x near the multicritical concentration. For the most Mn-rich sample ($x=0.35$), the small-angle scattering is well described by a single Lorentzian. The corresponding inverse ferromagnetic correlation length κ remains nonzero (less than 0.04 $Å^{-1}$) at all temperatures. For $x=0.32$, the Lorentzian scattering profile persists. As T is reduced, κ decreases to a value indistinguishable from zero and subsequently increases, as it should for a ferromagnet which evolves into a reentrant spin-glass. For progressively smaller x, the scattering function at low temperatures shows increasing deviations from the Lorentzian form, and instead is consistent with a power law $Q^{-\alpha}$ with $2<\alpha<3$. These results are very similar to those found in other alloy series which display both ferromagnetic and spin-glass behavior. We argue that this power-law form of the spin correlations in the reentrant phase provides an important clue to the nature of the ferromagnet—spin-glass transition and the reentrant state itself. This leads us to a detailed heuristic model for the phase diagram and phase-transition behavior, including the reentrant phenomenon. The model is based on a decomposition, via the frustration mechanism, of spin systems with exchange interactions of random sign, into spin-glass-like and ferromagnetic networks. Many of the experimental results are explained in terms of random-field effects which arise when the ferromagnetic and spin-glass order parameters are coupled together.

I. INTRODUCTION

In 1975, Sherrington and Kirkpatrick[1] calculated the magnetic phase diagram for an Ising spin system with infinite range interactions selected from a Gaussian distribution with mean J_0 and standard deviation J. Not surprisingly, they found a paramagnetic (PM) to ferromagnetic (FM) transition for large values of J_0/J. For small J_0/J, they found a paramagnetic to spin-glass (SG) transition of the type described by Edwards and Anderson.[2] Finally, for J_0/J of order unity, they discovered that with decreasing temperature, the system underwent a PM-FM ordering transition followed by an FM-SG "disordering" transition. After this calculation was published, experimentalists identified several magnetic alloys which seemed to exhibit such "reentrant" spin-glass (RSG) behavior. Initially, many of the alloys in question were nonmagnetic metals with moderately dilute magnetic impurities, and consequently SG and RSG phenomena were thought to be unique to systems, such as $(Pd_{1-y}Fe_y)_{1-x}Mn_x$,[3] with strong Ruderman-Kittel-Kasuya-Yodisa (RKKY) interactions between distant spins. More recently, SG and RSG behavior has been observed in concentrated spin systems, including the dilute magnetic semiconductors $Eu_xSr_{1-x}S$,[4] the polycrystalline metals Fe_3Al_{1-x},[3] and the amorphous alloys $(Fe_{1-x}Mn_x)_{75}P_{16}B_6Al_3$.[5–8] These are systems where randomness in the sign of the exchange interactions is brought about by random alloying, although not necessarily with nonmagnetic impurities, of exchange-coupled ferromagnets. Other systems exhibiting FM-RSG-SG behavior are metallic ferromagnets diluted with nonmagnetic or weakly magnetic atoms to a concentration near the FM nearest-neighbor percolation threshold.[9,10]. This class includes $Fe_{1-x}Cr_x$, $Fe_{1-x}Au_x$, and $(Fe_{1-x}Ni_x)_{75}P_{16}B_6Al_3$. Thus SG and RSG phenomena are not peculiar to dilute systems of spins coupled via long-range RKKY interactions, but are common to a wide range of random alloys with competing interactions between spins.

To date, magnetization measurements have provided most of the evidence for the existence of RSG phases. However, because they must be performed in finite ap-

plied fields, such measurements do not necessarily prove that a well-defined FM-RSG phase transition can occur. Furthermore, they yield little microscopic information, especially about the spin-spin correlations in the RSG phase. While neutron scattering experiments do not share the sensitivity of bulk measurements, they can be performed in zero applied field and give microscopic information. Consequently, we have carried out a detailed neutron scattering study of a concentrated spin system, namely amorphous $(Fe_{1-x}Mn_x)_{75}P_{16}B_6Al_3$, near its FM-SG crossover.

We chose to study this particular alloy series for several reasons. Firstly, Yeshurun *et al.*[6] have characterized it extensively by magnetization measurements, which they analyzed assuming a scaling hypothesis where the transition temperatures as well as the associated critical exponents were treated as free parameters. The resulting phase diagram, which features a FM-SG-PM multicritical point at $x=x_{mc}=0.35$ and $T=T_{mc}=42$ K, is reproduced in Fig. 1. The ac susceptibility measurements of Geohegan and Bhagat[6] give the same FM-PM phase boundary, but indicate that the SG-FM line is displaced upwards by ~ 20 K with respect to the corresponding line found by Yeshurun *et al.* Secondly, because the amorphous $(Fe_{1-x}Mn_x)_{75}P_{16}B_6Al_3$ alloys are formed by rapid quenching from the melt, structural properties vary smoothly over the entire composition range and metallurgical clustering is unlikely. Finally, both the temperature and Fe concentration at the SG-FM multicritical point are relatively high, which suggests that the spin-density and exchange interactions are large enough to make inelastic neutron scattering studies fairly straightforward.

The principal evidence that $(Fe_{1-x}Mn_x)_{75}P_{16}B_6Al_3$ is characterized by competing exchange interactions is the phase diagram[6] (Fig. 1) itself. The pure-iron system with $x=0$ is a ferromagnet with $T_c=630$ K. If the Mn-Fe and Mn-Mn interactions were ferromagnetic, then the ferromagnetic state would persist for all x. If the interactions were either zero or very weak, we would expect T_c to decrease gradually with x, going to zero at $x\simeq 0.8$. Instead, T_c drops precipitously as x is increased, with the ferromagnetism vanishing for $x>0.35$. This can only be understood in terms of antiferromagnetic Mn-Fe and, presumably, Mn-Mn interactions.

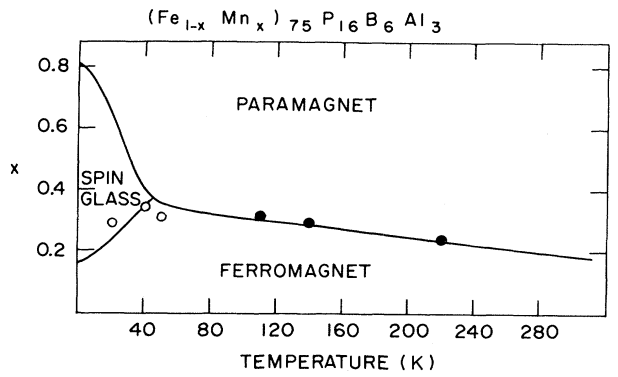

FIG. 1. Magnetic phase diagram of $(Fe_{1-x}Mn_x)_{75}P_{16}B_6Al_3$ from Ref. 6. Solid points represent our measured Curie temperatures; open circles, the lower temperatures at which the $Q=0.02$ Å^{-1} SANS intensity peaks (see Fig. 4).

In this and a planned future publication,[11] we present our quasielastic and inelastic neutron scattering experiments on $(Fe_{1-x}Mn_x)_{75}P_{16}B_6Al_3$. The current paper describes the quasielastic measurements performed for four manganese concentrations x near x_{mc}. In a preliminary report on our work,[8] we proposed a model for the FM-RSG transition. This model involves random-field effects, and is based on concepts borrowed from percolation theory. It accounts for features of both our data on $(Fe_{1-x}Mn_x)_{75}P_{16}B_6Al_3$, and similar results for other random magnetic alloys with competing interactions.[3–9] The aim of this paper is not only to give a complete description of our experimental data, but also to discuss, in more detail, our model for the FM-RSG crossover.

We turn now to the organization of this paper. Section II describes the experimental procedure, while Sec. III is concerned with the measured structure factors of the amorphous $(Fe_{1-x}Mn_x)_{75}P_{16}B_6Al_3$ samples. In Sec. IV, we present our data on the magnetic scattering near the forward direction. We note that Rainford and collaborators have collected data identical in many, but not all respects, for a very similar material, amorphous $(Fe_{1-x}Mn_x)_{80}P_{16}C_4$.[7] Section V contains a discussion of the random-field model for the FM-RSG crossover. In Sec. VI, we show how this model accounts for the experimental features of $(Fe_{1-x}Mn_x)_{75}P_{16}B_6Al_3$ and other systems. Finally, Sec. VII summarizes our findings and indicates directions for future research.

II. EXPERIMENTAL

A. Samples

The amorphous $(Fe_{1-x}Mn_x)_{75}P_{16}B_6Al_3$ ribbons used in our experiments were prepared by centrifugal quenching. Apart from the substitution of ^{11}B for the strongly absorbing isotope ^{10}B, these samples differ in no respect from those extensively characterized by ac susceptibility and dc magnetization measurements.[6] Approximately 5 g of the ribbon material were packed into a 1-cm-diam cylindrical aluminum sample holder, which in turn was mounted in a Displex cryostat (or flow Dewar for $x=0.65$) whose temperature could be regulated to better than 0.5 K between 9 and 350 K. Table I lists the samples studied, their transition temperatures, and the neutron scattering measurements performed on them. The alloy compositions cited are the concentrations of the melts from which the ribbons were formed. Therefore, they are to be regarded only as nominal compositions. Indeed, there are discrepancies of order 0.05 between these nominal values for x and the values obtained from electron microprobe measurements on $(Fe_{1-x}Mn_x)_{75}P_{16}B_6Al_3$ films.[6] Fortunately, the Curie temperatures of these alloys depend strongly on x (see Fig. 1), and consequently serve to identify—with little uncertainty—samples on the ferromagnetic side of the phase diagram.

TABLE I. Properties of $(Fe_{1-x}Mn_x)_{75}P_{16}B_6Al_3$ alloys used for our neutron scattering study. The last three columns indicate the types of neutron scattering measurements that we have performed.

	T_c			T_g			Neutron scattering measurements		
x[a]	bulk[b]	bulk[c]	SANS ($Q=0.02$ Å^{-1})	bulk[b]	bulk[c]	SANS ($Q=0.02$ Å^{-1})	SANS[d]	IENS[e]	ASF[f]
0.40									×
0.35[g]	42±2	none		42	42	42±10	×	×	×
0.32	100±2	104	88±3	32±2	63	50±3	×		
0.30	107±2	114	143±2	31±2	54	20±3	×	×	
0.25			221±1				×	×	×
0.20	293±4	280	340±5[h]	14±2	34			×	×

[a]Nominal concentrations, given by ratios between starting materials.
[b]Yeshurun *et al.* (see Ref. 6).
[c]Geohegan and Bhagat (see Ref. 6).
[d]Small angle neutron scattering (reported in this paper).
[e]Inelastic neutron scattering (to be described in a future paper).
[f]Amorphous structure factor (reported in this paper).
[g]Bulk measurements were reported for $x=0.34$.
[h]Measured on conventional triple-axis spectrometer for $Q=0.03$ Å^{-1}.

B. Neutron scattering technique

The experiments were carried out at the Brookhaven National Laboratory High Flux Beam Reactor (HFBR). We measured the amorphous structure factors using conventional triple-axis spectrometers. Pyrolytic graphite crystals, set for the (002) reflection, functioned as monochromators and analyzers. The spectrometers were operated in the elastic mode, with neutron energies $E=14.7$ or 48 meV.

By definition, no scattering function for an amorphous system, such as $(Fe_{1-x}Mn_x)_{75}P_{16}B_6Al_3$, is periodic in reciprocal space. Consequently, long-wavelength spin fluctuations must be probed near the forward direction. Because of their relatively poor vertical resolution, and complications due to the direct, unscattered beam, triple-axis spectrometers are not ideal for measurements of quasielastic scattering at small angles ($2\theta \lesssim 3°$). For our investigation of magnetic scattering, we have used a more suitable apparatus, namely the small-angle neutron scattering (SANS) spectrometer of the Brookhaven National Laboratory Biology Department. This instrument consists of a monochromator followed by a collimating tube with circular apertures at either end, and an 18×18-cm^2 wire chamber detector placed two meters beyond the sample. For the $x=0.25$ and 0.35 samples, we used a pyrolytic graphite monochromator. The incident neutron energy was 14.7 meV ($\lambda=2.36$ Å), and the resolution, measured from the direct-beam profile, was 0.006 Å^{-1} [halfwidth at half maximum (HWHM)]. For the $x=0.68$ and 0.70 samples, the spectrometer was installed at the cold neutron facility of the HFBR, and the incident beam was monochromated by an Fe-Mn multilayer with a d spacing of 73 Å and an uncertainty $\Delta d/d=0.08$ (HWHM). The neutron energy selected was 3.3 meV ($\lambda=5$ Å, and the Q resolution of the spectrometer was 0.003 Å^{-1} (HWHM) at $2\theta=0$. The data reported below are averages of the observed intensities taken over rings concentric with the beam incident on the detector. A cylindrical beamstop protected the detector from the direct beam and fixed the lower limit (0.012–0.025 Å^{-1}) on the range of momentum transfers over which useful data could be collected. Because this cutoff was always considerably higher than the resolution, resolution effects could be ignored in our analysis. Note that the combination of the circular collimator and the position-sensitive detector allowed us to avoid the difficulties caused by the substantial vertical divergence of ordinary triple- or double-axis spectrometers. Inelastic scattering measurements, performed on triple-axis spectrometers and to be described in a future paper,[11] justify the quasielastic approximation in the SANS studies of all four samples. This means that we are measuring the Fourier transform of the *instantaneous* spin-correlation function. Thus, the observed magnetic scattering is proportional to

$$\frac{d\sigma}{d\Omega}=\int\frac{\partial^2\sigma}{\partial\Omega\,\partial\omega}d\omega\sim\sum_{l,m}\langle\vec{S}_l\cdot\vec{S}_m\rangle\exp[i\vec{Q}\cdot(\vec{r}_l-\vec{r}_m)]\ . \tag{1}$$

In Eq. (1) the spins $\vec{S}_l$ are located at the sites $\vec{r}_l$ and $\vec{Q}$ is the scattering vector.

III. AMORPHOUS STRUCTURE FACTOR

Figure 2 displays the measured structure factors for three samples. Two of these ($x=0.40$ and 0.35) are on the spin-glass side of the phase diagram (see Fig. 1 and Table I), while the last ($x=0.20$) is the most iron-rich sample that we have studied and is on the ferromagnetic side. No Bragg peaks can be seen in Fig. 2, which confirms that our samples are truly amorphous. A large maximum

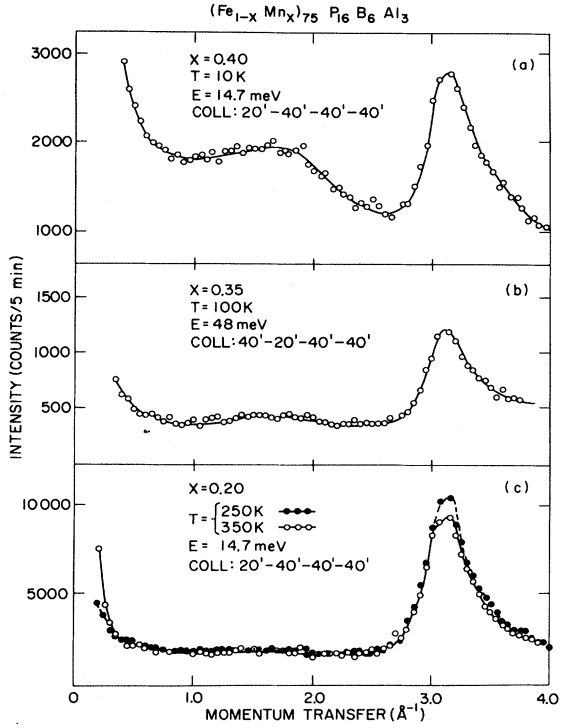

FIG. 2. Amorphous structure factor measured for $(Fe_{1-x}Mn_x)_{75}P_{16}B_6Al_3$.

occurs at a wave vector $Q \simeq 3.1$ Å^{-1} close to that of the lowest-order reflection (110) of crystalline (bcc) iron. With increasing x, a maximum also develops at $Q \simeq 1.7$ Å^{-1}. One possible cause is short-range antiferromagnetic order; note that the spectrum for $x=0.40$ [Fig. 2(a)], where the maximum is most pronounced, was collected at 10 K. Upon warming to 200 K, the maximum is reduced by less than 15%, and spin-polarized neutron scattering measurements[12] show that the spectra at room temperature are almost entirely accounted for by processes not involving a neutron spin flip. Therefore, the maximum at $Q \simeq 1.7$ Å^{-1} is due primarily to positional correlations between the Fe and Mn atoms in the amorphous solid. The neutron scattering technique is particularly sensitive to such correlations because the scattering lengths of Fe and Mn are of opposite sign: $b_{Fe}=0.96$ and $b_{Mn}=-0.37\times10^{12}$ cm.[13] In contrast, Fe and Mn have nearly identical x-ray scattering lengths because they are neighbors in the Periodic Table.

Figure 2(c) shows spectra taken at temperatures T above (350 K) and below (250 K) the measured Curie point $T_c=325$ K for $x=0.20$. As T is reduced through T_c there are two important changes in the spectra: (a) The scattering near the forward direction ($Q<0.5$ Å^{-1}) decreases, and (b) the maximum at $Q \simeq 3.1$ Å^{-1} grows. (a) corresponds to the reduction in spin fluctuations as ferromagnetic order sets in. (b) is due to ferromagnetic-order-parameter scattering, which, quite generally, is proportional to the Fourier transform $\rho(\vec{Q})$ of the pair-correlation function for the magnetic species. Recall that in a crystalline substance, $\rho(\vec{Q})$ consists of a set of δ functions centered at reciprocal-lattice points. On the other hand, in amorphous solids such as $(Fe_{1-x}Mn_x)_{75}P_{16}B_6Al_3$, $\rho(\vec{Q})$ is a smooth function with its first maximum at $2\pi/a$, where a is a suitably defined mean interatomic spacing.

IV. SANS DATA

A. Constant-Q temperature scans

Figure 3 shows the temperature dependence of the scattered neutron intensity at momentum transfers $Q=0.02$ and 0.03 Å^{-1}. For the most Mn-rich [$x=0.35$, see Fig. 3(a)] compound, there is little change as a function of temperature, and the principal feature of the data is a broad maximum centered near 40 K, which is approximately where the phase diagram of Yeshurun *et al.*[6] (Fig. 1) would place the SG transition. As x is decreased to 0.32 [Fig. 3(b)] the data evolve much more dramatically with changing T. In addition to a broad maximum which occurs at consistently lower temperatures as Q is increased, there is now an anomaly, barely visible in Fig. 3(b), for all values of Q at $T=88\pm3$ K. The data for $x=0.30$ [Fig. 3(c)] are qualitatively similar; here the upper anomaly has developed into a well-defined peak at $T=143\pm2$ K, while the lower maximum is more intense and has moved to lower temperatures. Finally, for $x=0.25$ [Fig. 3(d)], we see a sharp maximum at $T=221\pm1$ K, and a dramatic increase in the scattered intensity at temperatures below 80 K.

In Table I the characteristic temperatures given by in-

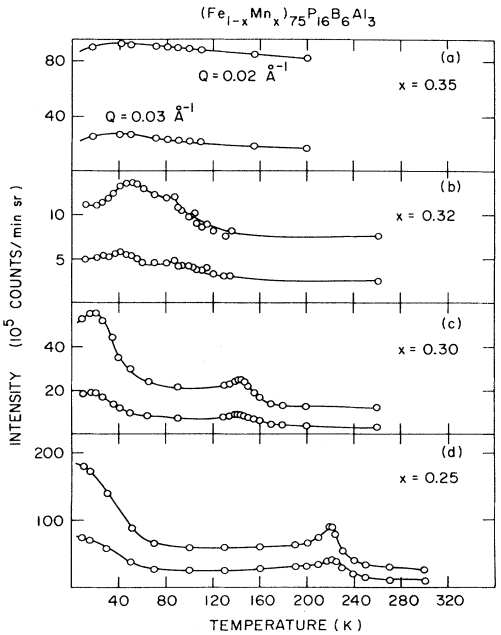

FIG. 3. Temperature dependence of SANS intensity for $Q=0.02$ and 0.03 Å^{-1}. No background corrections have been made.

spection of our SANS data are compared to the bulk transition temperatures. The high-temperature anomalies for the samples with $x \leq 0.32$ represent the critical scattering associated with PM to FM transitions in these materials. Indeed, the corresponding temperatures T_c, indicated by the filled circles in Fig. 1, fall near the PM-FM phase boundary deduced from the earlier scaling analysis of the magnetization measurements.[6]

Because the positions $T_l(Q)$ of the low T maxima in Fig. 4 change with Q, we cannot with certainty extract lower critical temperatures $T_l^0 = T_l$ $(Q=0)$ to compare with the RSG transition temperatures found by other techniques. However, assuming that $T_l(Q)$ continues to increase with decreasing Q, we can use our $Q=0.02$ Å^{-1} data (Fig. 3) to place lower limits of 50 and 20 K on T_l^0 for $x=0.32$ and 0.30, respectively. These bounds are indicated by open circles in Fig. 1. For $x=0.32$, $T(Q=0.02)$ Å^{-1} falls between the values of T_g obtained directly from the susceptibility measurements of Geohegan and Bhagat, and those extracted in the scaling analysis of Yeshurun *et al.*,[6] while for $x=0.30$, it is below the results of both bulk experiments.

B. Q dependence of the scattered intensity

We emphasize that the data of Fig. 3 are raw in the sense that no attempt has been made to correct for nonmagnetic background scattering. To estimate the Q dependence of the magnetic scattering, such correction is essential and we have followed the standard procedure of subtracting as background the highest temperature spectra collected at each x. Figures 4 and 5 show the resulting inverse intensities $I^{-1}(Q)$ plotted vs Q at various temperatures. On such plots, Lorentzian scattering profiles

$$I(Q)=\frac{A}{\kappa^2+Q^2} \tag{2}$$

reduce to straight lines, with slopes A^{-1} and intercepts

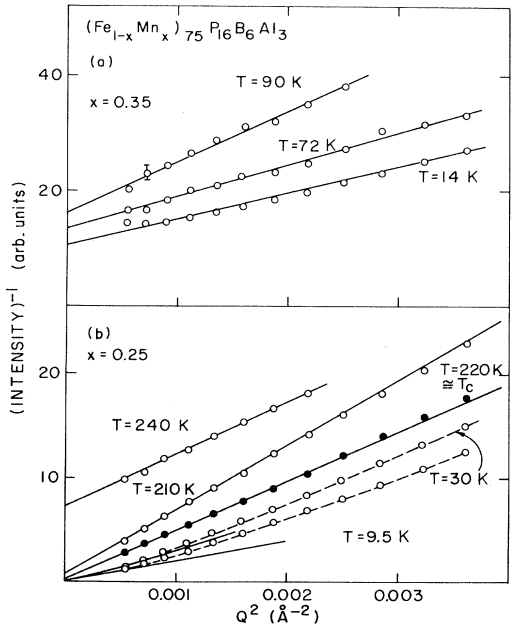

FIG. 4. Inverse intensity I^{-1} vs Q at various temperatures for (a) $x=0.35$ and (b) $x=0.25$, the two samples studied using neutrons with an incident energy $E_i=14.7$ meV. The $T=200$- and 350-K spectra were taken as background for the $x=0.35$ and 0.25 data, respectively. The dashed line through the $T=9.5$-K data ($x=0.25$) represents a $Q^{-2.6}$ power law.

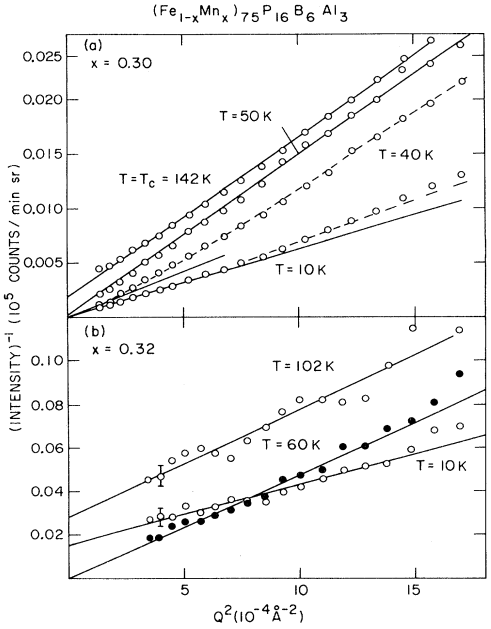

FIG. 5. Inverse intensity I^{-1} vs Q^2 for (a) $x=0.30$ and (b) $x=0.32$, the two samples studied using cold neutrons ($E_i=3.3$ meV). Background spectra were taken at $T=330$ and 250 K for $x=0.30$ and 0.32, respectively.

reduce to straight lines, with slopes A^{-1} and intercepts

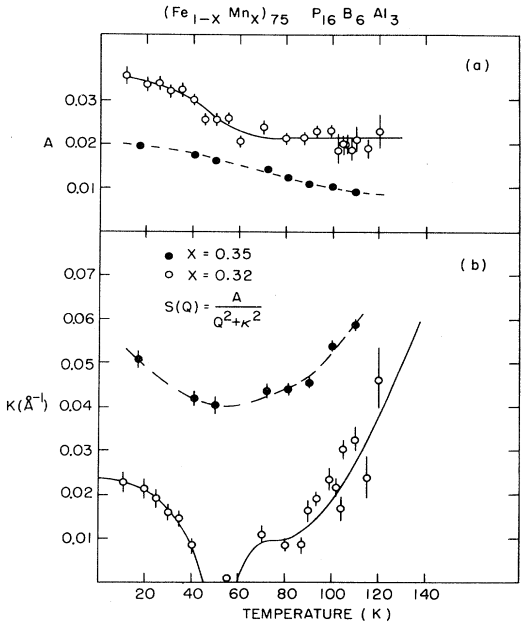

FIG. 6. Temperature dependence of inverse correlation length κ and Lorentzian amplitude A for $x=0.35$ (open circles) and $x=0.32$ (closed circles).

$-\kappa^2$. For $x=0.35$, Eq. (2) always gives an excellent description of the data. Figure 6 shows the temperature dependence of the amplitude A and the FM inverse correlation length $\kappa=\xi^{-1}$, obtained from least-squares fits of Eq. (2) to the data. These results should not be considered quantitatively exact because the background was collected at a relatively low temperature (200 K). Even so, it is clear that ξ remains finite for all T and reaches a maximum of ~ 25 Å near $T=50$K.

As is evident from Fig. 5(b), the Lorentzian form Eq. (2) also describes the low-Q ($Q<0.04$ Å^{-1}) data for $x=0.32$. However, κ and A undergo very different T-dependent evolutions (see Fig. 6) compared with that for $x=0.35$. Notably, as T is lowered, κ first decreases to 0.01 Å^{-1} at $T_c\approx 88$ K, the temperature at which the upper anomalies in the constant-Q scans [Fig. 3(b)] occur. Only subsequently, for $45<T<60$ K, does κ seem to vanish, as it should in a normal Heisenberg ferromagnet below its Curie point T_c. With further decreases in T, κ *increases* monotonically so that at 10 K, the FM correlation length $\xi<50$ Å. The temperature dependence of the amplitude A is equally peculiar. For $T>60$ K, A remains constant as in a normal ferromagnet *above* T_c.[14] There is a substantial increase in A near 50 K followed by a gradual increase at the lowest temperatures. As we shall discuss later in this paper, the fact that κ does not appear to go to zero at T_c may be an artifact due to a distribution of T_c's in the sample; however, we believe that all of the other observed phenomena are intrinsic features of FM-RSG systems.

Figure 5(a) shows typical spectra for $x=0.30$, while Fig. 7 displays the temperature dependence of the Lorentzian fitting parameters. At high temperatures, these data are quite similar to those for $x=0.32$. The magnetic scattering is considerably more intense, but κ still reaches a nonzero minimum at the nominal FM-PM transition. The amplitude behaves more as in a normal FM: A remains constant for $T>T_c$ while it decreases noticeably for $90<T<T_c$. For all $T<50$ K, κ is indistinguishable from zero (i.e., $\kappa<0.005$ Å^{-1}). Furthermore, in this temperature range, the observed $I(Q)$ shows clear deviations from the Lorentzian form Eq. (2), represented by solid lines in Fig. 5(a). Indeed, power-law singularities $Q^{-\alpha}$, with $\alpha\geq 2$ describe these data more adequately, as indicated by the dashed lines in Fig. 5(a). Figure 8 shows the temperature dependence of the exponent α where α was varied freely in fits to the data. Note that the deviations from the standard Q^{-2} form are most severe not at the lowest temperatures, but at $T\simeq 30$ K.

For $x=0.25$, the high-temperature ($T>160$ K) data again obey Eq. (2) [see Figs. 4(b) and 7]. In this case, however, κ does become indistinguishable from zero at T_c. Below T_c, κ increases slightly with decreasing T, while for $T\leq 160$ K, it remains zero to within experimental error. Consistent with the notion that this material is a ferromagnet below $T_c=221\pm 1$ K, the amplitude $A(T)$ decreases below T_c. However, $A(T)$ always remains larger than $A_{SW}(T)=\frac{2}{3}A(T_c)T/T_c$ where $A_{SW}(T)$ is the standard spin-wave–dominated fluctuation amplitude associated with Heisenberg ferromagnets.[14] Indeed, for $T<90$ K, A increases again, and the scattering profile shows even greater deviations from the $1/Q^2$ law than for $x=0.30$: At the lowest temperatures, the data are well represented by a power law $Q^{-\alpha}$ where $\alpha\simeq 2.5$. Unlike the behavior for $x=0.30$, the fitted exponent α, indicated by the solid circles in Fig. 8, increases monotonically with decreasing temperature for $x=0.25$.

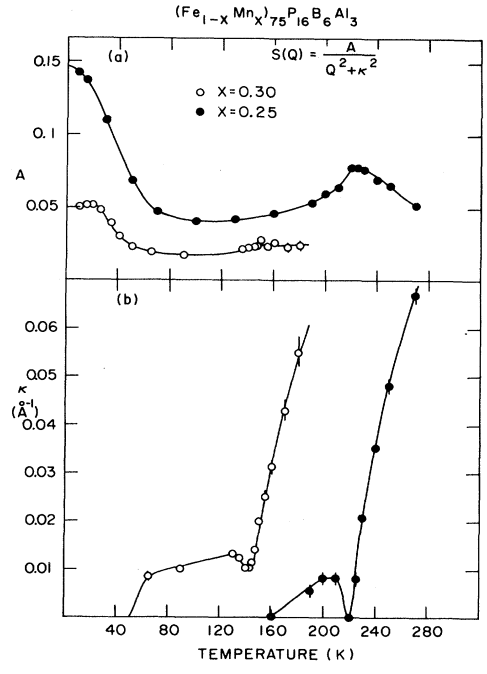

FIG. 7. Temperature dependence of inverse correlation length κ and Lorentzian amplitude A for $x=0.30$ (open circles) and $x=0.25$ (closed circles).

V. DISCUSSION: RANDOM FIELDS AND THE FM-RSG CROSSOVER

A. Introduction

To begin, we summarize our experimental findings and compare them to the results of measurements on other

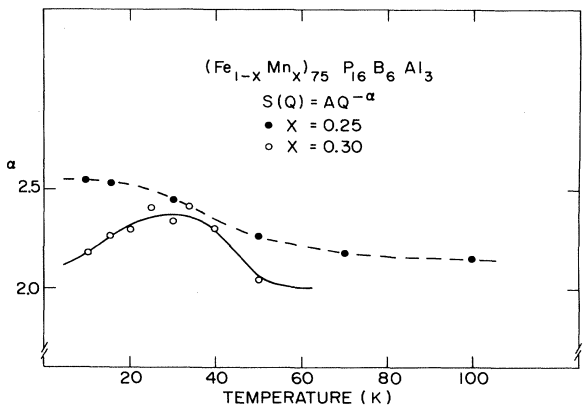

FIG. 8. Temperature dependence of exponent α in power-law fit to the data for $x=0.30$ and 0.25.

random magnetic systems. Firstly, there is an anomaly in the critical scattering at the ferromagnetic transition, but the inverse correlation length κ does not appear to go to zero. This behavior is commonly observed in random alloys[7,15] and in most cases is believed to originate simply from a spread on T_c's. This does not, of course, rule out mechanisms intrinsic to FM-SG-RSG systems. Secondly, deviations from the Lorentzian form [Eq. (2)] for the scattering profile are seen at low temperatures, and the deviations are larger for the more ferromagnetic samples. SANS measurements on $Eu_xSr_{1-x}S$,[14] Fe_xCr_{1-x},[10] and PdFeMn (Ref. 16) yield similar results. Thirdly, for the FM sample ($x=0.32$), where the Lorentzian form holds at all T, the inverse FM correlation length κ is indistinguishable from zero for intermediate T and increases monotically as T is reduced below a certain temperature. Rainford *et al.*[7] have not observed this in $(Fe_{1-x}Mn_x)_{80}P_{16}C_4$, but a recent neutron scattering study has revealed analogous behavior in $Eu_{0.52}Sr_{0.48}S$.[4]

As we have just described, the neutron scattering results for $(Fe_{1-x}Mn_x)_{75}P_{16}B_6Al_3$ are very similar to those for other random magnetic alloys, some of which are neither amorphous nor metallic. The same is true of the available bulk susceptibility data. The remarkable universality of the empirical results for RSG alloys suggests that the explanation for these results must be quite general and rely on the feature common to all RSG alloys, namely magnetic interactions which are random in sign. Many calculations of RSG behavior invoke infinite-range interactions to facilitate computations.[17] This approach is adequate for model systems, but in our view, is highly unlikely to describe real concentrated spin systems like $(Fe_{1-x}Mn_x)_{75}P_{26}B_6Al_3$ and $Eu_xSr_{1-x}S$, where the short-range interactions are both large and random in sign. In particular, we believe that local geometric effects are an essential feature of the RSG phenomenon and an infinite-range model cannot possibly contain such effects. In two previous papers[4,8] we gave brief descriptions of a model which takes competing short-range interactions into account. For RSG behavior to occur within this model, a true SG phase—in the Edwards-Anderson sense—need not exist. The only stipulation is that the relaxation rates for certain spins must become anomalously small as the temperature is reduced. This requirement can be met because both experiments on real materials and computer simulations[18] of *short-range* spin glasses show that the SG "phase" is characterized by hysteresis effects and long relaxation times.

In this section, we present our model and its experimental consequences in greater detail. The discussion is organized as follows. Borrowing concepts from magnetic percolation theory,[19] we first review how frustration allows a decomposition of the spin system into FM and SG networks.[20,21] In the following sections, the consequences of the coupling between the two networks are explored.

B. Decomposition of spin system into FM and SG parts

Let us review briefly the percolation problem, where magnetic ions occupy a random fraction p of the sites in some nonmagnetic host.[19] If these ions are coupled only via short-range interactions, there will be a percolation threshold $p_c \geq 0$ such that for $p < p_c$, the ions will exist in finite clusters, isolated magnetically from each other (Fig. 9). Thus, the range of spin correlations is also finite, and the system can never display a net magnetic moment. On the other hand, if $p \geq p_c$, an infinite connected network of spins does exist, and consequently a macroscopic moment can develop at low temperatures. Even so, finite spin clusters, decoupled from the infinite network by intervening nonmagnetic ions, persist if $p \neq 1$. As p approaches p_c from above, the fraction of spins in such clusters approaches unity, that is, all the spins are in decoupled clusters and the long-range order disappears.

In systems with competing exchange interactions, it is also possible to isolate clusters of spins from each other. The decoupling mechanism is frustration, illustrated in Fig. 10, which is not as simple as bond percolation. We start with an ordered, square ferromagnet and replace a small number of positive exchange bonds with negative bonds of equal magnitude. Figure 10(a) shows a particularly simple bond configuration which can result. The spin in the center is frustrated—no direction is favored—because it has zero net coupling to its ferromagnetic environment. Figures 10(b) and 10(c) show how larger clusters of spins can be similarly decoupled from ferromagnetic surroundings. The classical ground states of these clusters, when considered by themselves, are ferromagnetic. It is also possible to consider decoupled clusters which include negative exchange bonds and consequently have nonferromagnetic ground states [Fig. 10(d)]. In general, we state that a spin cluster is decoupled from its FM environment if the interfacial energy is invariant with respect to global (uniform) rotations of a ground state of the cluster. This means that an equal number of positive and negative bonds must join the cluster spins to the FM spins. A

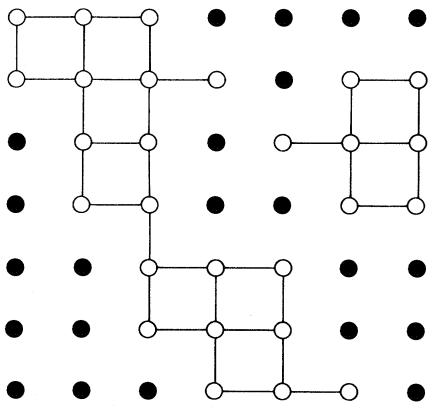

FIG. 9. Magnetically decoupled clusters in the percolation problem with nearest-neighbor exchange.

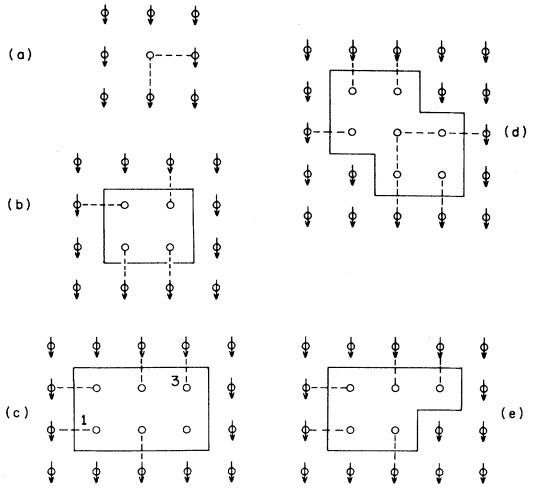

FIG. 10. Spins frustrated with respect to FM environment: single spin (a), multispin clusters with FM ground state [(b), (c), and (e)], cluster with nonferromagnetic ground state (d). Dashed lines correspond to antiferromagnetic couplings; all other nearest-neighbor pairs are coupled ferromagnetically. Note that the bond configurations in (c) and (e) are the same.

stronger form of decoupling entails invariance of the interfacial energy with respect to local (position-dependent) rotations of the spins inside the cluster. Clusters (a), (b), and (d) differ from (c) in that they are decoupled in this local sense. Such local rotations generate excited states of the clusters.

With frustration decoupling in mind, we define four thresholds, analogous to p_c in the percolation problem, that can be crossed by the concentration x of negative exchange bonds introduced into an otherwise ferromagnetic system. The first, $x_{\rm SG}$, will correspond to the percolation threshold for spins $\vec{\sigma}_i$ belonging to "decoupled" clusters, and the second, $x_{\rm FM}$, to the concentration beyond which it becomes impossible to define an infinite FM network of unfrustrated spins $\vec{S}_j$. The third and fourth are merely the antiferromagnetic analogs of $x_{\rm FM}$ and $x_{\rm SG}$. In certain real RSG alloys, such as $Eu_xSr_{1-x}S$, the ratio of positive to negative bonds is changed by introducing nonmagnetic constituents into a ferromagnet. This means that these alloys will display no crossover from spin glass to antiferromagnetic behavior. Instead, the spin-glass region of the phase diagram will be bounded by the ordinary magnetic percolation threshold x_p. In crystalline $Eu_xSr_{1-x}S$, the onset of SG behavior occurs at $x=0.14$, which indeed is the next-nearest-neighbor percolation threshold for an fcc lattice.[4]

As we discussed previously,[8] the above concept of frustration decoupling was motivated by the computer simulations of Binder *et al.*[20] More recently Barahona *et al.*[21] have studied in some detail the ground states of frustrated 2D Ising models as a function of the negative bond concentration. Their results show clearly the generation of decoupled clusters by the frustration mechanism. They also show that in finite systems (20×20) there are extended boundaries where the net interaction is weak but negative, causing the spin direction to change sign across the boundary. Maynard and Rammal[21] argue that these antiphase boundaries may generate a stable "random antiphase state" at low temperatures. We believe that this state will be difficult to distinguish from SG and RSG states, especially when one incorporates the random-field effects discussed below.

C. Coupling between SG and FM networks

We now consider the case where x is between $x_{\rm SG}$ and $x_{\rm FM}$. Here there are two infinite connected networks: The first contains spins $\vec{S}_i$ coupled ferromagnetically while the second only has *finite* connected FM subnetworks containing spins $\vec{\sigma}_j$. The corresponding Hamiltonians are

$$H_F=-\sum_{i,j}J_{ij}\vec{S}_i\cdot\vec{S}_j\ , \tag{3}$$

with $J_{ij}\geq 0$, and

$$H_S=-\sum_{i,j}I_{ij}\vec{\sigma}_j\cdot\vec{\sigma}_j\ . \tag{4}$$

H_F, taken by itself, is the Hamiltonian for a ferromagnet with Curie temperature T_c. Similarly, H_S describes a spin glass which undergoes freezing near a temperature T_g. Figure 11 shows schematically how T_g and T_c might vary with (a) the concentration of negative exchange bonds randomly substituted for positive bonds of equal magnitude, and (b) a nonmagnetic ion concentration in a real alloy such as $Eu_xSr_{1-x}S$. The $T=0$ thresholds $x_{\rm FM}$, $x_{\rm SG}$, $x_{\rm ASG}$, $x_{\rm AFM}$, and x_p are as defined in Sec. V B above. We note parenthetically that the decomposition of a system with exchange bonds of random sign into SG and FM networks is not necessarily unique. Figures 10(c) and 10(e), which show two ways of apportioning spins to an FM network and a "decoupled" cluster, illustrate this point. However, it is probable, but unproven, that the temperatures $T_c(x)$ and $T_g(x)$ do not depend upon the particular decomposition chosen. We take this view primarily because of the recent work of Maynard and Rammal on two- and three-dimensional Ising models with exchange interactions of random sign.[21] Also, the computer simulations of Binder *et al.*[20] on $Eu_xSr_{1-x}S$ give $T_c(x)$ and $x_{\rm FM}$ in excellent agreement with bulk measurements, where random-field effects are suppressed by applied fields.[4]

In the percolation problem, the spin clusters are decoupled from each other by virtue of physical separation, and so the net Hamiltonian is merely the sum of the Hamiltonians for the decoupled clusters—both finite and infinite—in the system. The problem of mixed exchange interactions is different, because here the net Hamiltonian H_N includes bonds joining the FM network to the frustrated clusters of spins $\vec{\sigma}_j$. Therefore, there must be a coupling term,

$$H_C=-\sum_{i,j}K_{ij}\vec{\sigma}\cdot\vec{S}_j\ , \tag{5}$$

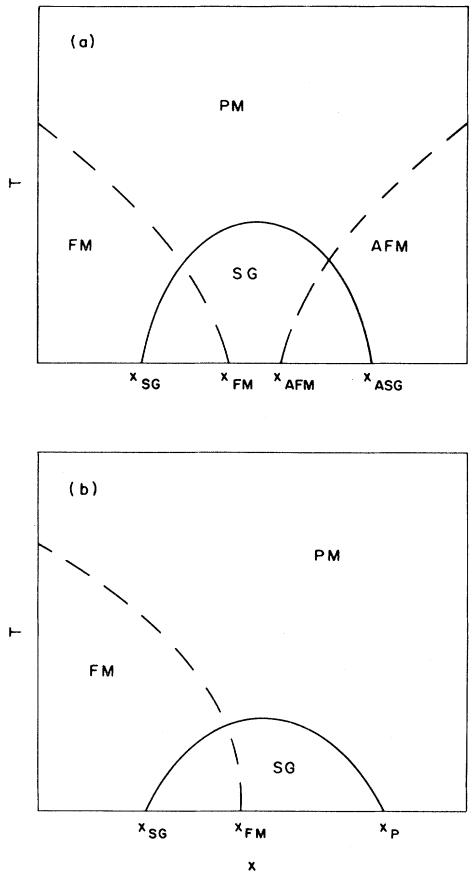

FIG. 11. Schematic phase diagram for RSG alloy. In (a) x is the concentration of negative exchange bonds, in (b), x is a nonmagnetic ion concentration. Dashed and solid curves represent transition temperatures for spin-glass and antiferromagnetic networks, respectively.

in the decomposition

$$H_N = H_F + H_S + H_C \ . \tag{6}$$

It should be emphasized that in the percolationlike alloy systems such as $Fe_{1-x}Cr_x$ and $(Fe_{1-x}Ni_x)P_{75}B_6Al_3$ there will be long-range RKKY interactions both between the "isolated" clusters and between the clusters and the infinite network. In the percolating insulator $KMn_xZn_{1-x}F_4$,[15] dipolar interactions couple the clusters to each other and the infinite network. Thus H_C is nonvanishing in spin systems which exhibit RSG behavior near their ordinary percolation thresholds.

We now consider the effect of H_C in the limits where either the spins $\vec{S}_i$ are ferromagnetically ordered or the SG spins $\vec{\sigma}_i$ are frozen. In the first case,

$$H_C = \vec{M} \cdot \sum_{i,j} \vec{\sigma}_j K_{ij} \ , \tag{7}$$

where $\vec{M} = \langle \vec{S}_i \rangle_T$ is the net magnetization.

By the definition of our decoupling scheme, H_C is invariant with respect to uniform rotations of an SG ground state $\{\sigma_i^G\}$. Thus, collective freezing among the $\vec{\sigma}_i$ can still occur in the presence of H_C. This should also be true where the effective field from H_C is nonzero, but much less than kT_g. However, because H_C may break the degeneracy between $\{\sigma_i^G\}$ and other SG ground states not related to $\{\sigma_i^G\}$ by some uniform rotation, the freezing transition here will typically have different properties than when the $\vec{\sigma}_i$ are isolated from the FM network. Notably, the characteristic temperature will be shifted from T_g to T_g'; it seems likely that due to the decreased ground-state entropy brought about by H_C, $T_g' > T_g$.

We now turn to the opposite limit where an SG transition has taken place and the spins $\vec{\sigma}_i$ are frozen. The coupling H_C can be rewritten as

$$H_C = \sum_i \vec{S} \cdot \vec{h}_i \ , \tag{8}$$

where

$$\vec{h}_i = \sum_j \langle \vec{\sigma}_j \rangle K_{ij} \ . \tag{9}$$

In other words, H_C acts to impose a *random field* on the FM network. Recent theory and experiments[22–24] indicate that the presence of a random-field term is equivalent to a reduction in the spatial dimensionality of the system by two. In particular, an infinitesimally small random field will destroy long-range FM order in a three-dimensional short-range-coupled Heisenberg magnet. To understand the effects of a random field on the spin-correlation function and its Fourier transform $S(\vec{Q})$, recall first that for an ordered Heisenberg system,

$$S(\vec{Q}) = A\delta(\vec{Q}) + \tfrac{2}{3}S_\perp(\vec{Q}) + \tfrac{1}{3}S_{||}(\vec{Q}) \ . \tag{10}$$

In Eq. (10) the coefficient A is directly proportional to the square of the order parameter (e.g., the magnetization for a ferromagnet). The transverse fluctuations are spin waves, and accordingly, $S_\perp(Q) \sim Q^{-2}$. Finally, $S_{||}$ accounts for the longitudinal spin fluctuations. Ordinarily, $S_{||}$ is well described by a Lorentzian of width κ_l; κ_l grows from zero as T is reduced below T_c. One may write the Q dependence explicitly:

$$S(\vec{Q}) = A\delta(\vec{Q}) + \frac{B}{Q^2} + \frac{C}{Q^2+\kappa_l^2} \ . \tag{11}$$

Based on heuristic arguments as well as experimental results for Ising systems,[23,24] imposition of a random field on a system with spatial dimensionality $d \leq 4$ converts $S(\vec{Q})$ in Eq. (10) to

$$S'(\vec{Q}) = \frac{A'}{(Q^2+\kappa^2)^2} + \frac{A''+B'}{Q^2+\kappa^2} + \frac{C'}{Q^2+\kappa_l'^2} \ . \tag{12}$$

The relationship between κ_l' and κ is not known at present. From the perspective of ordinary critical phenomena, where scattering functions take the form $Q^{-(2-\eta)}$ with η small but positive, the most unusual feature of Eq. (12) is the presence of the Lorentzian squared "order-parameter" term. Not so surprising is the Lorentzian "spin-wave" term $B'(Q^2+\kappa^2)^{-1}$, since over lengths short compared to κ^{-1}, the system still appears ferromagnetic. We include a mathematically redundant coefficient A'' to emphasize

that the random field converts the δ-function order-parameter scattering of Eq. (10) into the *sum* of a Lorentzian and its square. A simple domain-wall argument[22] shows that the random-field-induced inverse correlation length,

$$\kappa \sim \langle \mid h_i \mid^2 \rangle^{1/(4-d)} . \tag{13}$$

If we require the Lorentzian squared term in Eq. (12) to become the δ-function term in Eq. (11) as $\vec{h}_i \to 0$, we find that

$$A' \sim \mid \vec{M} \mid^2 \kappa^{4-d} , \tag{14}$$

where $\vec{M}$ is the magnetization for $\vec{h}_i = \vec{0}$. This has been confirmed experimentally in both $Rb_2Co_xMg_{1-x}F_4$ and $Co_xZn_{1-x}F_2$.[24] To interpret data, it is useful to know that for fixed Q and A', and varying κ, the Lorentzian squared term in Eq. (12) has a maximum when $\kappa = Q/\sqrt{3}$.

D. Phase diagram and FM-SG crossover

In the previous section, we discussed the consequences of the coupling H_C between FM and SG networks in the limits of frozen FM and SG order. The important conclusions were that SG order can destroy FM order, while FM order can change the nature of the SG transition. Consequently, for general spatial dimensionality d, it makes sense to speak of renormalized (by H_C) critical temperatures T_g' and T_c' corresponding to T_g and T_c. We now describe what happens in the x-T plane for $d=3$ in terms of these characteristic temperatures T_g' and T_c', which can be defined at each x.

In general, if $T < T_g'$ the SG will impose on the FM network an effective random field with mean-square amplitude directly proportional to the Edwards-Anderson order parameter q_{EA}:

$$\langle \mid \vec{h}_i \mid^2 \rangle \sim (zJ)^2 \langle \mid \vec{\sigma}_i \mid^2 \rangle \sim (zJ)^2 q_{EA} . \tag{15}$$

The quantity z measures the fraction of spins $\vec{S}_i$ coupled to the SG network via (positive and negative) exchange bonds of average magnitude J. As $x \to x_{FM}$, the FM network contains vanishingly few spins and $z \to 1$. There are two cases to consider.

(1) $T_c < T_g'$. Because of the random-field effects, there cannot be any FM transition at any temperature, and so T_c' is undefined. The experimental behavior will be the same as that expected when a random field is applied to a pure FM above its Curie point. The scattering profile will be predominantly Lorentzian and, with decreasing T, the inverse correlation length κ will decrease towards a minimum at some T_0 where $T_0 < T_g'$; depending on the explicit concentration, κ may actually increase again for $T < T_0$ as the random fields increase in strength.

(2) $T_c' > T_g'$. FM order can develop for $T_c' > T > T_g'$, while for $T < T_g'$, it will be destroyed and κ will grow from zero according to a formula like Eq. (13). Close to the multicritical point defined by $T_c' = T_g'$, the scattering should be predominantly Lorentzian, as when $T_c' < T_g'$. However, as $T_c' - T_g'$ becomes larger, the Bragg scattering at low temperatures should include a correspondingly larger Lorentzian-squared component. Furthermore, the coupling zJ in Eq. (15) between the SG and FM networks will be weaker, and so the random-field-induced width κ will become immeasurably small. The resulting SANS spectra will have the form

$$S'(\vec{Q}) = \frac{a}{(Q^2+\kappa^2)^2} + \frac{b}{Q^2+\kappa^2} , \tag{16}$$

which over a relatively wide range of $Q > \kappa$ is difficult to distinguish from

$$S'(Q) = AQ^{-\alpha} , \tag{17}$$

with $2 < \alpha < 4$. Indeed in the two-dimensional and three-dimensional random-field Ising systems all of the data for $Q \gtrsim 2\kappa$ are well represented by Eq. (17), with α varying between about 2.3 and 3.5, depending on the relative amplitudes of the Lorentzian and Lorentzian-squared terms.[24] In Heisenberg systems, the weight of the Lorentzian is enhanced because of spin waves. Interpretation of the neutron scattering profiles for RSG alloys is further complicated by large but finite FM clusters embedded in the SG network. However, it seems reasonable to assume that $S'(\vec{Q})$ for small $\vec{Q}$ is dominated by the FM network for $x \ll x_{FM}$, and by the large finite clusters for $x \geq x_{FM}$. This is in agreement with work on the magnetic percolation problem,[19] and is also justified by the relatively low SANS intensities observed for samples on the SG side of FM-SG-PM multicritical points.[10]

There is another important issue related to the decomposition into FM and SG networks. In the magnetic percolation problem, clusters of ions are decoupled by virtue of intervening nonmagnetic ions, independent of the magnetic order within the clusters. The frustration decoupling scheme described above is different in that the SG spins $\vec{\sigma}_i$ are decoupled from the FM network only when the latter is fully ordered. This means that when random-field effects set in, decoupling can be accomplished only on length scales less than the FM correlation length. Note that if we change the definition of the FM network to allow for the spin correlations within it to decay over a finite distance ξ, the fraction $f(\xi)$ of spins in the "FM" network would increase. This may cause the anomalous rise at low temperatures in the Lorentzian amplitude A [see Eq. (2)] for several RSG alloys, including $Eu_xSr_{1-x}S$ (Ref. 4) and $(Fe_{1-x}Mn_x)_{75}P_{16}B_6Al_3$ near their FM-SG-PM multicritical points.

We have concentrated on the zero-field properties of RSG systems because the neutron scattering technique gives convenient access to these properties. Bulk measurements, however, are performed in applied dc and ac fields.[4,7,9] Here we make the simple observation that a field comparable in magnitude to the terms $h_i = \sum_j K_{ij} \langle \vec{\sigma}_j \rangle$ in H_C [see Eq. (8)] will supress the random-field effects described above. An important result is that in the presence of an external field H, the spin system will behave as if the effective Curie temperature T_c' were higher, and its effective spin-glass temperature T_g' lower. For temperatures near T_g', $\mid \vec{h}_i \mid$ is small, with the result that small, nonzero H can lead to qualitative changes in magnetic behavior. Sensitivity of the apparent phase diagram to small H is a feature common to many

RSG alloys, including Fe_xCr_{1-x},[9] $Eu_xSr_{1-x}S$,[4] and $(Fe_{1-x}Mn_x)_{75}P_{16}B_6Al_3$.[6] Rosenbaum *et al.*[5] have pointed out that with increasing applied field, SG and RSG systems might exhibit behavior analogous to that associated with the depinning of charge-density waves.

Until now, we have referred to a finite Edwards-Anderson order parameter q_{EA} below a well-defined SG transition temperature. However, the FM order will be unstable with respect to the random field induced by the $\vec{\sigma}_i$ as long as the SG relaxation time τ exceeds the domain-formation time for the FM network. This has important consequences for the FM-RSG crossover, which occurs as τ grows with decreasing temperature. Namely, the crossover should take place at a temperature higher than the SG transition temperature T_g, defined by $\tau \rightarrow \infty$. How far above T_g this happens can only be determined from a detailed theory. In any case, it is interesting that one real alloy, namely Fe_3Al_{1-x}, apparently exhibits a reentrant (paramagnetic) transition before undergoing an SG transition, marked by the usual cusp in the ac susceptibility.[25] In addition, the SANS spectra deviate from Lorentzian behavior at temperatures near the so-called inverse Curie temperature.[26] Of course, reentrant behavior can occur even in the absence, at all temperatures, of a true SG phase.

VI. DISCUSSION: APPLICATION OF RANDOM-FIELD MODEL TO $(Fe_{1-x}Mn_x)_{75}P_{16}B_6Al_3$

In the previous section we have given a detailed discussion of a heuristic model for the FM-SG crossover. Our objective here is to describe how this model accounts for many features of the SANS data for $(Fe_{1-x}Mn_x)_{75}P_{16}B_6Al_3$.

For the sample with the lowest Fe content ($x=0.35$) the scattering profile is Lorentzian at all temperatures. In addition, the inverse correlation length κ passes through a smooth minimum near the SG transition temperature established by bulk measurements (see Table I). These results are easily understood in terms of our random-field model, if we say that the transition temperature T_g for the decoupled SG network is higher than the Curie point T_c for the FM network. As discussed previously, a separation between the two networks is no longer possible. Furthermore, as the temperature is lowered through T_g, the growing effective random field breaks up the finite correlated FM regions and thus leads to an increase in κ. Clearly, this is only a consistency argument showing that the data can be reconciled with our model.

Our most Mn-rich alloy ($x=0.32$) on the ferromagnetic side of the phase diagram displays much more complicated behavior. The inverse correlation length appears to vanish below the nominal Curie temperature $T_c' \approx 88$ K, and then increases again for $T < T_g' \sim 50$ K. The latter is, of course, exactly what should happen in the presence of a growing effective random field. Many spins belong to the SG network in this sample, and T_g' and T_c' are not very different. Also, the FM order is not well developed for $T \gtrsim T_g'$, with the result that the SANS profiles are predominantly Lorentzian at all temperatures. The rise in the scattering amplitude A for low T is caused by the incorporation of SG spins $\vec{\sigma}_i$ in correlated FM regions as the FM network is fractured by random-field effects. We note again, however, that finite FM clusters embedded in the SG network can complicate this scenario, and in particular, enhance the Lorentzian nature of the SANS profiles.

We now turn to the behavior near T_c'. The simplest cause of the nonzero κ at T_c' is a spread in T_c' due to macroscopic inhomogeneities in the Mn concentration x. Specifically, if T is set at the median T_c' then regions of the sample with $T > \langle T_c' \rangle$ and $T < \langle T_c' \rangle$ will both exhibit critical scattering with a finite κ. This leads to SANS with a nonzero κ throughout the smearing region. The subsequent rise in κ then is due to the longitudinal fluctuation terms in Eq. (11). Finally, at lower temperatures the spin-wave term will dominate over the unusually large longitudinal critical scattering term $c/(\kappa_l^2+Q^2)$, and the SANS κ will therefore appear to go to zero. Concentration nonuniformities of order 0.25% are sufficient to account for the value of κ at T_c. This is also true for the $x=0.30$ sample. Surprisingly, for $x=0.25$, κ does become indistinguishable from zero at T_c, which means either that the Mn concentration is more uniform in this sample, or that the observed behavior near T_c is due to subtle random-field effects.[27]

We emphasize that our experiment, where the FM order parameter is not measured, is also consistent with the absence of an FM transition to true long-range order for $x=0.32$. Instead, the state could be characterized by a power-law singularity. As in $Eu_{0.52}Sr_{0.48}S$, which displays very similar spin fluctuations but *no* δ-function magnetic Bragg scattering,[4] a small applied dc field would be sufficient to eliminate the random-field effects above T_g and cause this alloy to behave as if it were truly ferromagnetic.

For $x=0.30$, the behavior is similar to that for $x=0.32$, although there are some important differences in detail (see Figs. 3, 7, and 8). A larger percentage of spins resides in the FM network, so that the RSG transition occurs at a lower temperature $T_c' \gtrsim 20$. Also, the FM order is correspondingly more developed for $T_g' < T < T_c' \approx 143$, and the random-field strength lower for $T < T_g'$, which leads to deviations from simple Lorentzian behavior for $T < T_g'$.

Finally, for $x=0.25$ the scattering is dominated by the FM network, both pseudo-Bragg and diffuse. In this case the SANS intensities for $Q=0.02$ and 0.03 Å^{-1} rise continuously with decreasing T. This implies that the random-field-induced κ is of order 0.01 Å^{-1} or less. Indeed, a power-law form $AQ^{-\alpha}$ with α increasing substantially as T is reduced, fits the SANS spectra very well.

Figure 12 shows the lowest-temperature (9.5 K) data collected for $x=0.25$. The solid line represents the power law $Q^{-2.54}$ which best fits these data, while the dashed line corresponds to the random-field form (16) with $\kappa=0.015$ Å^{-1} and $\kappa^2 b/a=0.13$. Note that for $Q^2 < 0.006$ Å^{-2}, the two functions describe the data equally well. Over the entire range of momentum transfers, the power-law fit appears to be somewhat better. Both of these results have also been found in the neutron scattering work on the random-field problem.[24] The discrepancy at larger Q between Eq. (16) and the data

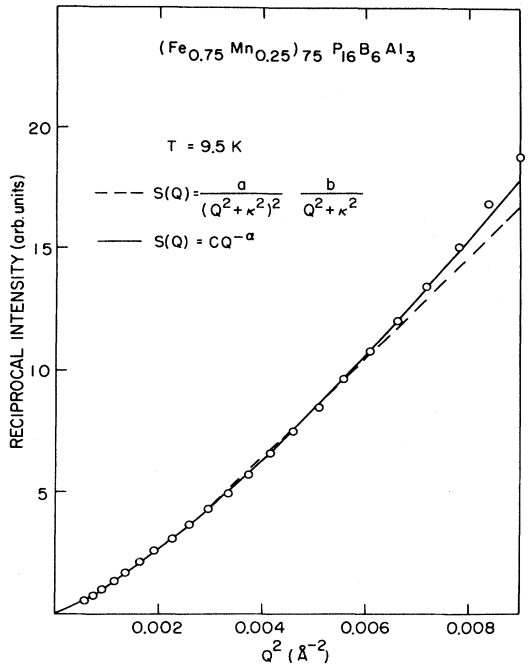

FIG. 12. Comparison of power law ($\alpha=2.54$) and random-field forms ($\kappa=0.015$ Å^{-1}, $\kappa^2 b/a=0.13$) which best fit the low-temperature data for $x=0.25$.

could well be due to the harmonic approximation used in deriving Eq. (16).[22]

VII. SUMMARY AND CONCLUSIONS

We have performed quasielastic neutron scattering measurements on amorphous $(Fe_{1-x}Mn_x)_{75}P_{16}B_6Al_3$ for concentrations x near the crossover from ferromagnetism to spin-glass behavior. As x is decreased from 0.35, the magnetic scattering intensity near the forward direction increases dramatically, and its profile at low temperatures evolves from a Lorentzian $(Q^2+\kappa^2)^{-1}$ with $\kappa\neq 0$ to a power-law singularity $Q^{-\alpha}$ with $\alpha>2$.

We have given a detailed discussion of a model which accounts for many of the anomalous features of not only our own data on $(Fe_{1-x}Mn_x)_{75}P_{16}B_6Al_3$, but similar results in a wide variety of other systems including $Eu_xSr_{1-x}S$, $Fe_{1-x}Cr_x$, and $KMn_xZn_{1-x}F_4$. Among these results are non-Lorentzian scattering profiles and finite correlation lengths at low T. We emphasize that within our model, RSG behavior can occur even in the absence of a true SG transition in the Edwards-Anderson sense; the principal requirement is an imbalance in the relaxation times for different spin clusters in the system.

In conclusion, we stress that our model is primarily phenomenological. Indeed, it is based on heuristic notions about the statistical geometry of frustrated spins and random-field effects in Heisenberg systems. Our simple two-component factorization will require further elaboration. In addition, further progress on the random-field problem is clearly a prerequisite for a more quantitative understanding of RSG systems.

ACKNOWLEDGMENTS

It is a pleasure to acknowledge A. N. Berker, K. Binder, S. Bhagat, R. Bruinsma, R. Cowley, P. Horn, J. Lynn, H. Maletta, B. Rainford, T. Rosenbaum, M. Salamon, W. Saslow, D. Sherrington, H. Sompolinsky, G. Shirane, and H. Yoshizawa for helpful discussions of this work. We thank Y. Fujii for performing x-ray diffraction measurements on our samples, and G. Shirane for sharing with us spin-polarized neutron scattering data on $(Fe_{0.60}Mn_{0.40})_{75}P_{16}B_6Al_3$. Finally, we are very grateful to D. Schneider for valuable assistance in the SANS experiments, and D. Carlson for helpful comments on the data analysis. The work at Brookhaven National Laboratory was supported by the Division of Material Sciences, U.S. Department of Energy under Contract No. E-AC02-76CH00016. The work at the Massachusetts Institute of Technology was supported by the National Science Foundation Low-Temperature Physics Program under Contract No. DMR-79-23203.

[1]D. Sherrington and S. Kirkpatrick, Phys. Rev. Lett. 35, 1792 (1975).

[2]S. F. Edwards and P. W. Anderson, J. Phys. F 5, 965 (1975).

[3]For a review of work on polycrystalline metals exhibiting RSG behavior, see G. J. Nieuwenhuys, B. H. Verbeek, and J. A. Mydosh, J. Appl. Phys. 50, 1685 (1979).

[4]H. Maletta, J. Appl. Phys. 53, 2185 (1982); H. Maletta and W. Felsch, Z. Phys. B 37, 55 (1980); H. Maletta, G. Aeppli, and S. M. Shapiro, Phys. Rev. Lett. 48, 1490 (1982).

[5]T. F. Rosenbaum, L. W. Rupp, Jr., G. A. Thomas, W. M. Walsh, Jr., H. S. Chen, J. R. Banavar, and P. B. Littlewood, Solid State Commun. 42, 725 (1982); T. F. Rosenbaum, L. W. Rupp, G. A. Thomas, H. S. Chen, J. R. Banavar, and C. M. Varma (unpublished).

[6]Y. Yeshurun, M. B. Salamon, K. V. Rao, and H. S. Chen, Phys. Rev. B 24, 1536 (1981); J. A. Geohegan and S. M. Bhagat, J. Magn. Magn. Mat. 25, 17 (1981).

[7]B. D. Rainford, J. R. Davis, and W. Howarth, in *Neutron Scattering—1981, Argonne National Laboratory,* Proceedings of the Conference on Neutron Scattering, edited by J. Faber, Jr. (AIP, New York, 1982), p. 239.

[8]G. Aeppli, S. M. Shapiro, R. J. Birgeneau, and H. S. Chen, Phys. Rev. B 25, 4882 (1982).

[9]S. M. Shapiro, C. R. Fincher, A. C. Palumbo, and R. D. Parks, Phys. Rev. B 24, 6661 (1981); J. W. Lynn, R. W. Erwin, J. J. Rhyne and H. S. Chen, J. Appl. Phys. 52, 1738 (1981); B. V. B. Sarkissian, J. Phys. F 11, 2191 (1981).

[10]S. K. Burke, R. Cywinski, J. R. Davis, and B. D. Rainford, J. Phys. F 13, 441 (1983); 13, 451 (1983); 13, 471 (1983).

[11]G. Aeppli, S. M. Shapiro, R. J. Birgeneau, and H. S. Chen (unpublished).

[12]G. Shirane, private communication.

[13]G. E. Bacon, *Neutron Diffraction* (Clarendon, Oxford, 1975).
[14]See J. Als-Nielsen, O. W. Dietrich, and L. Passell, Phys. Rev. B 14, 4908 (1976), and references therein.
[15]R. A. Cowley, G. Shirane, R. J. Birgeneau, E. C. Svensson, and H. J. Guggenheim, Phys. Rev. B 22, 4412 (1980).
[16]S. M. Shapiro, G. Shirane, B. H. Verbeek, G. J. Nieuwenhuys, and J. A. Mydosh, Solid State Commun. 36, 167 (1980).
[17]M. Gabay and G. Toulouse, Phys. Rev. Lett. 47, 201 (1981), and references therein; D. Bowman and J. W. Halley, Phys. Rev. B 25, 1892 (1982).
[18]See, for example, W. Kinzel, Z. Phys. B 46, 59 (1982), and references therein.
[19]R. J. Birgeneau, R. A. Cowley, G. Shirane, J. A. Tarvin, and H. J. Guggenheim, Phys. Rev. B 21, 317 (1980).
[20]K. Binder, W. Kinzel, and D. Stauffer, Z. Phys. B 36, 161 (1979).
[21]F. Barahona, R. Maynard, R. Rammal and J. P. Uhry, J. Phys. A 15, 673 (1982); R. Maynard and R. Rammal, J. Phys. (Paris) Lett. 43, L347 (1982).
[22]Y. Imry and S.-k. Ma. Phys. Rev. Lett. 35, 1399 (1975); G. Parisi and N. Sourlas, *ibid.* 43, 744 (1979), and references therein; E. Pytte, Y. Imry, and D. Mukamel, *ibid.* 46, 1173 (1981); D. Mukamel and E. Pytte, Phys. Rev. B 25, 4775 (1982).
[23]H. S. Kogon and D. J. Wallace, J. Phys. A 14, L527 (1981).
[24]H. Yoshizawa, R. A. Cowley, G. Shirane, R. J. Birgeneau, H. J. Guggenheim, and H. Ikeda, Phys. Rev. Lett. 48, 438 (1982); R. J. Birgeneau, H. Yoshizawa, R. A. Cowley, G. Shirane, and H. Ikeda, Phys. Rev. B 28, 1438 (1983).
[25]R. D. Shull, H. Okamoto, and P. A. Beck, Solid State Commun. 20, 863 (1976).
[26]H. R. Child, J. Appl. Phys. 52, 1732 (1981); K. Motoya, S. M. Shapiro, and T. Muraoka, in Proceedings of the Yamada Conference VI—Neutron Scattering of Condensed Matter, 1982 (in press).
[27]G. Aeppli, Ph.D. thesis, Massachusetts Institute of Technology, Cambridge, Massachusetts, 1982 (unpublished).